EXPERIMENTAL APPROACH TO FLOW FIELD EVALUATION IN UPPER PLENUM OF REACTOR VESSEL FOR INNOVATIVE SODIUM COOLED FAST REACTOR

N. Kimura, K. Hayashi, H. Kamide

Japan Atomic Energy Agency, Oarai Research and Development Center

Abstract

In Japan Atomic Energy Agency, an innovative sodium cooled fast reactor of 1500MWe class, JSFR, has been investigated on the Fast Reactor Cycle Technology Development project. A compact reactor vessel (R/V) and a column type upper inner structure with a radial slit for an arm of a fuel-handling machine are adopted. These result in increase of the spatial-averaged velocity on the horizontal cross section of the R/V by factor of 2.5. These high velocities may cause gas entrainment at the free surface in the upper plenum and also the cavitations. Therefore horizontal dipped plates (D/P) are set below the free surface to prevent the gas entrainment. We performed two water experiments using an 1/10th scaled full-sector model of the upper plenum of R/V and a large scaled partial model. The flow optimization in the upper plenum was performed in the full-sector model. It was observed in the large scaled model that the gas entrainment occurred under the extreme velocity conditions which were far from the rated condition in the reactor design of JSFR. Consequently, there is a chance for this design of the compact reactor vessel to suppress the gas entrainment and cavitation.

1. INTRODUCTION

In fast reactors, an improvement of cost performance is of importance as well as safety. In Japan Atomic Energy Agency (JAEA), various types of fast reactors have been investigated as the Fast Reactor Cycle Technology Development (FaCT) project (Kotake, 2008). In the FaCT project, an advanced loop type sodium cooled fast reactor with 1500MWe class core (JSFR) has been investigated (Shimakawa, 2002). A design study is undergoing for this plant. Figure 1 shows the overview of the JSFR. The reactor system is simplified to reduce construction cost, so as to compete with a future commercial light water reactor and also to keep safety. For example, thermal output is increased against the reactor size, an intermediate heat exchanger and a main primary pump are united, number of the primary loops is decreased from three or four to two, and so on. As for an upper plenum of reactor vessel (R/V), a single rotation plug and a fuel-handling machine (FHM) with a swing type arm are adopted to simplify the fuel handling system. A column type upper inner structure (UIS), which consists of control rod guide tubes, six horizontal perforated plates, and has no outer cover, has a radial slit in the horizontal plates for the arm of the FHM to move inside the UIS and access all subassemblies. The diameter of the R/V can be reduced by using this UIS concept with the slit. There is no need of space to move out the UIS from the core top during a fuel handling. Coolant passes through the inside of the UIS to increase mixing volume in the upper plenum and to mitigate thermal transient after a scram. There is a free surface in the upper plenum of the R/V to keep a deck at lower temperature. As compared with Japanese Demonstration Fast Breeder Reactor (DFBR) in the design study (Ueta, 1995), core flow rate increases as thermal output increases by factor of 2.5, while the diameter of the R/V is nearly equal. These result in increase of the spatial-

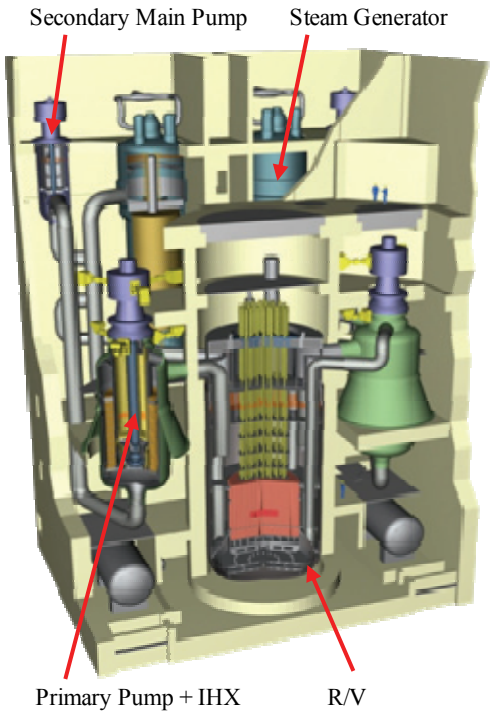

Figure 1 Overview of JSFR.

averaged velocity on the horizontal cross section of the R/V by factor of 2.5. This large amount of coolant is sucked into two hot leg (H/L) intakes; the average velocity in the H/L pipe reaches 9.2m/s. These high velocities may cause gas entrainment at the free surface in the upper plenum and also the cavitations. So the dipped plates (D/P) are set up below the free surface to prevent the gas entrainment. And cover gas above the free surface is pressurized at 0.25MPa (absolute pressure). However, there are many gaps between the D/P and the H/L piping and also between the D/P and the R/V, etc. Further, flow velocity passing through the UIS slit will be very high, comparable with core outlet velocity, ~5m/s. Eguchi (1994-1) showed the gas entrainment phenomena depended on circulation at the free surface and downward flow velocity for the stable vortex. The downward flow in the gap of D/Ps may generate the gas entrainment. In the study for DFBR, some experiments were carried out for an intermediate heat exchanger with the free surface (Eguchi, 1994-2). These experimental apparatuses had different scales (1/8th, 1/3rd, 1/1.6th) and the same geometry. It was observed in the experiments that actual vortex travelled at the free surface and the gas entrainment occurred intermittently. Further, it was found that the onset condition of gas entrainment depended on the model scale. These results suggested that a large-scaled experiment was needed to evaluate the onset condition of gas entrainment in the reactor and the onset condition of gas entrainment was conservative under the velocity similarity condition as in the reactor.

We performed an 1/10th scaled model water experiment for the upper plenum in the R/V. The objective of the study is flow optimization in the upper plenum to have prospects of the compact reactor vessel. Flow fields in the upper plenum are evaluated by using visualization, the particle image velocimetry (PIV) (Adrian, 1991) and the ultrasound velocity profile monitor (UVP) (Takeda, 1990). And other hydraulic problems are also picked up. After then, we investigate suitable structures to control the flow in the upper plenum. Furthermore, a large-scaled water experiment was performed to investigate dominant factors (e.g. downward velocity, horizontal velocity, etc) and the mechanism of the gas entrainment.

2. EXPERIMENT

2.1 Design of JSFR

Figure 2 shows the R/V of the JSFR in the design at the end of FY2001. The diameter of the core is 6580mm, and the inner diameter of the R/V is 9700mm. The primary cooling system consists of two loops, and each loop has one hot leg (H/L) pipe and two cold leg (C/L) pipes in the upper plenum of the R/V. These two H/L and four C/L pipes are put into the upper plenum from the top. In addition, two cold traps (C/T), which purify sodium, and a dipped heat exchanger (DHX), which removes the decay heat in the reactor, are installed in the upper plenum of the R/V. The H/L intakes are set at the middle height in the upper plenum. The C/Ls pass through the upper plenum. The upper inner structure (UIS) is set up above the core to insert control rods into the core and to measure subassembly outlet temperature. The UIS consists of six perforated plates and 55 control rod guide tubes. Sodium can flow inside the UIS to increase the mixing volume during a transient (The column type UIS). The lowest perforated plate is named the hold down plate (HDP), and the other five plates are named the baffle plates (B/P). The diameters of the HDP and the B/P are approximately 5000mm and correspond to the driver core region excluding the blanket and the reflector regions. All of the HDP and the B/Ps have the radial slit in order to pass through the arm of the fuel-handling

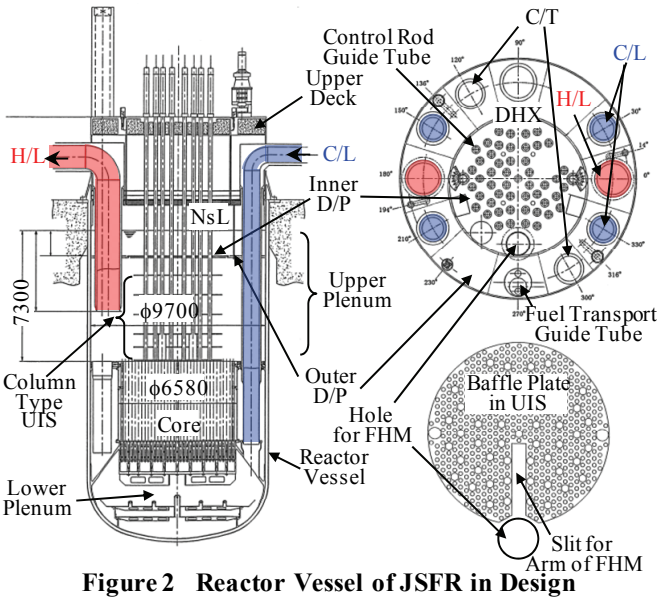

Figure 2 Reactor Vessel of JSFR in Design at the end of FY2001.

machine (FHM). The widths of the slits in the HDP and the B/P are 345mm and 385mm, respectively. The HDP and the B/P have a hole above each of the fuel subassembly. The diameter of the hole is slightly larger than the subassembly outlet.

The dipped plates (D/P) are set at 1400mm below the free surface to prevent sodium flow from impinging on the free surface. The D/Ps are divided into the inner and the outer ones. The inner D/P can rotate with the UIS during the fuel handling. The inner and the outer D/Ps consist of double plates in order to reduce the flow velocity in the gaps.

There are many gaps between the inner and the outer D/Ps, between the D/P and the components in the upper plenum, between the D/P and the R/V wall to prevent the structural damages due to the flow-induced vibration, thermal expansion, and so on. Therefore, the labyrinths formed like 'horseshoe' or 'L character' are set at the gaps region to restrict flow passing through the gaps.

2.2 Experimental Apparatuses

Figure 3 shows an experimental apparatuses of the 1/10th scaled R/V upper plenum model and the 1/1.8th scaled partial model. As for the 1/10th scaled model, the model scale was decided so as to change geometry easily and to find suitable one, when we considered the design phase of the reactor system was still early one. The geometry of the R/V upper plenum was modelled correctly with 1/10th scale including the inner components. The diameter of the upper plenum in the experimental apparatus is 1.0m. In the upper plenum, the UIS, two H/Ls, four C/Ls, two C/Ts, a DHX, a fuel transport guide tube and the inner and the outer D/Ps are set up as well as in the reactor. The D/Ps are modelled as a single plate in the experiment in order to estimate the velocity toward the free surface conservatively. Almost of all components in the upper plenum are made of transparent materials, e.g., acrylic resin to visualize flow pattern and to measure local velocity using optical methods. In the reactor design, there is a hole to insert the FHM through the inner D/P in the direction of the UIS slit as shown in Fig. 2.

In the study on gas entrainment in the IHX for the DFBR (Eguchi, 1994-2), water experiments were carried out using four scaled models from 1/10th to 1/1.6th scale. Dependence of the scale and the velocity condition were estimated for the onset of the gas entrainment. It was shown that the onset condition of the gas entrainment was the same velocity condition as in the reactor through the four scaled models and the experimental apparatus should be a larger than 1/3rd scale in order to evaluate the onset condition of gas entrainment quantitatively. Therefore we determined that the experimental apparatus had 1/1.8th scale against the reactor in this study. In the preliminary evaluation, upward flow was observed in front of the UIS slit and downward flow around the H/L in the region above the D/Ps. It is noted that downward flow is one of dominant factors for the gas entrainment. The 1/1.8th scaled test section modelled the 90 degree sector of the R/V with a central focus on the H/L circumferentially and region above the D/Ps vertically. The boundary condition in the 1/1.8th scaled model is given by the measured velocities in the 1/10th scaled upper plenum model. In the 1/10th scaled model, local velocities were measured under Froude number similarity condition. The measured results were applied to the 1/1.8th scaled model by extrapolation to the reactor condition. The experiments using two experimental models are undergoing with tight interaction. The test

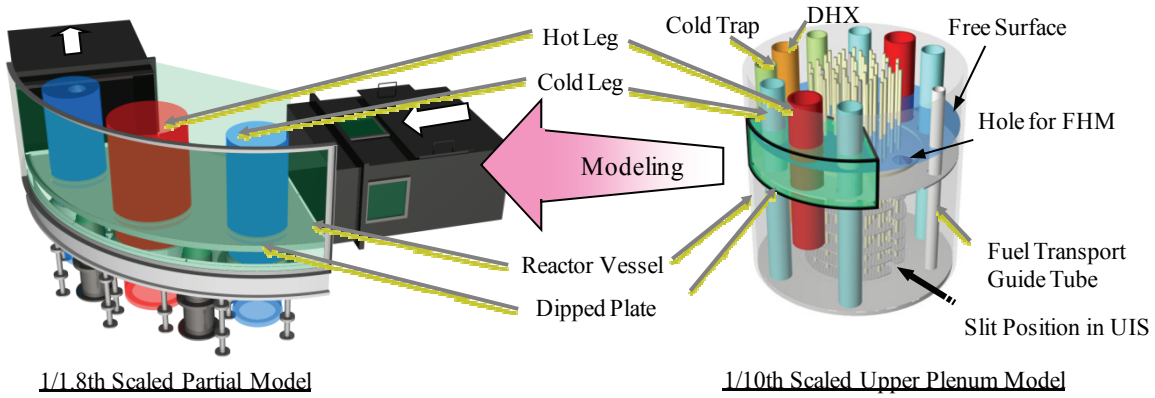

Figure 3 1/10th scaled upper plenum model and 1/1.8th scaled partial model.

section of the 1/1.8th scaled model consists of a rectangular tank with 4000mm(W) × 2000mm(D) × 2000mm(H). The faces of the rectangular tank are made of acrylic resin in order to visualize flow field. A simulated R/V wall made of polycarbonate plate with 2mm thickness is set up in the rectangular tank to reduce an effect of refraction for the velocity measurement using optical techniques. One H/L, two C/Ls and the D/Ps are installed in the test section and these components are also made of acrylic resin. In the preliminary evaluation, it was found that circumferential flow near the H/L above the D/Ps came from the UIS slit side and went to the opposite side (the DHX side). Therefore, two horizontal flow channels are set up in both sides of the rectangular tank of the 1/1.8th model to simulate the circumferential flow. The channel in the UIS slit side (right side) can make tangential inlet flow to the test section, and the channel in the DHX side can make tangential outlet flow. In the apparatus, the flow boundaries are set at the gap of D/Ps and the radial cross sections at both sides. Flow velocity as the boundary conditions in the radial cross sections at both sides are given by the two horizontal flow channels.

2.3 Experimental Conditions

The objective of this study is the flow optimization in the upper plenum of the R/V, e.g., prevention of the gas entrainment at the free surface, cavitations, and flow instability, etc. In the 1/10th scaled model, the flow similarity including the free surface is dependent on the Froude (Fr) number and the Reynolds number (Re). The effect of the Re number on flow field will be small under a larger Re condition. Thus, we mainly performed the experiment under the Fr number similarity condition.

The Fr number is defined as follows;

$$Fr = V/\sqrt{gL} \quad (1).$$

Here, V is the outlet velocity of the core, and L is the diameter of the R/V. In the experiment under the Fr number similarity condition, the core outlet velocity is $1/\sqrt{10}$ times smaller than that in the reactor. And the same velocity condition as in the reactor was also examined to see the occurrence of gas entrainment and cavitation qualitatively. The experimental apparatus used water as working fluid, temperature was 15 ~ 30 degree Celsius. The flow rate at the blanket region was set at 5% of total flow rate; flow velocity was 12% of that in driver fuel.

Figure 4 shows the boundary velocity condition of the 1/1.8th scaled model. This figure includes also nozzles configuration in the test section. The nozzles of the gaps are divided into 90 degree sector around the H/L, 180 degree sector around the C/Ls, 30 degree sectors at the gaps between the inner and outer D/Ps, and between the R/V and the outer D/P. All of the nozzles are attached to the bottoms of the D/Ps to reduce leak flow and clarify the boundary velocity condition. These velocities were extrapolated from the experimental data obtained by using the Particle Image Velocimetry (PIV) and the Ultrasound Doppler Velocity Profile Monitor (UVP) under Froude number similarity condition in the 1/10th model after the flow optimization. The plus value means the flow into the test section, and the minus value means the flow out of the test section. The velocities obtained from the PIV and the UVP were averaged in time, 10s and 70s, respectively. The downward flow was observed around the H/L pipe. The downward flows were also seen around the C/L pipes in the H/L side, the R/V gap and the gap between the inner and outer D/Ps near the H/L. In the geometry of double D/Ps, the sodium level from the top of D/P is 1400mm under the rated condition in the reactor. In the single D/P geometry, it is necessary to add the thickness of eliminated D/P and the clearance between the D/Ps to 1400mm and therefore the sodium level is 1510mm. In the 1/1.8th partial model, the water level corresponding to the designed reactor is 835mm under the rated condition.

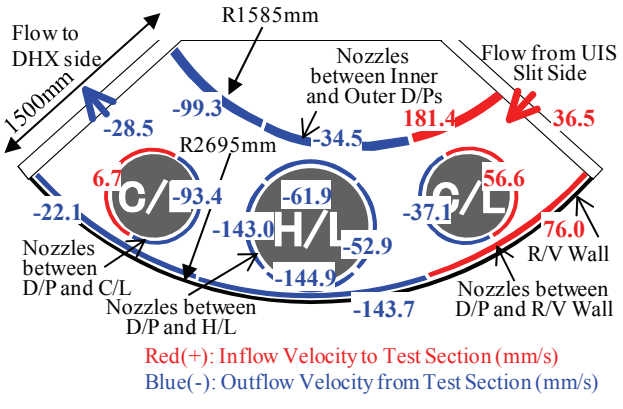

Figure 4 Flow Nozzles Configuration and Boundary Velocity Condition.

Table 1 Experimental Condition of 1/1.8th Scaled Model.

	Downward Velocity at D/P Gap (W)	Circumferential Velocity from UIS Slit side(V)	Water Level (L)
(1) Experiment for Occurrence Map of Gas Entrainment			
Ratio*	1~4	1~8	0.84~0.12
(2) Velocity Measurement at Region between R/V Wall and H/L			
Ratio*	1.5	2.1	0.24

*Ratio: Ratio of averaged velocity or coolant level in the test section to the reactor condition

Table 1 shows the experimental parameters in the study. The circumferential velocity, the downward velocity and the water level were varied widely to investigate the dominant factors for the gas entrainment (refer to Table 1 (1)). Thereby occurrence maps for the gas entrainment were constructed. In the occurrence map, there were two kinds of the gas entrainment as described in Section 3.3. Therefore the velocity measurement was performed using the PIV to investigate flow field, which caused the gas entrainment, in the pattern.

2.4 Measurement Techniques of Flow Field

At first, we performed flow visualization using a tuft method and small bubble injection method to grasp the qualitative flow pattern in the R/V upper plenum. The bubble behavior was affected by buoyancy force because the typical diameter of bubble was around one millimeter. So we used the bubble injection method at the high velocity region only. Quantitative velocities were obtained using the particle image velocimetry (PIV) and the ultrasound velocity profile monitor (UVP).

The PIV is one of optical measurements based on image processing techniques to get instantaneous and spatial velocity profile. Recently, the PIV has been applied to the velocity measurement with complex geometry by advances of image processing. Our PIV system was based on cross-correlation method with sub-pixel accuracy (Sakakibara, 1993). And noise reduction techniques (Kimura, 2000) for the visualized images were applied in order to reduce the error velocity vectors near the structures. The laser sheet, generated by a double-pulsed Nd-YAG laser system, was inserted into the apparatus. Nylon particles were used as seeding, the diameter was approximately 30~50μm. And a CCD camera, which could capture 30 images per second, was set in the normal direction to the laser sheet. The pixel number of the camera was 1008 (horizontally; H) x 1018 (vertically; V), and the size of the image was approximately 150mm (H) x 150mm (V). The spatial resolution of the velocity measurement was 3mm. The typical measured error was 0.03m/s. The measured region in the model was subdivided and the images were captured in the multiple regions by moving the CCD camera and the laser sheet. The time interval of the velocity measurement was 0.067s and the number of the data was 300 or 600 (10s or 20s) at one position.

The UVP is a non-contact measurement technique of flow velocity based on ultrasound Doppler shift. The emitted ultrasound beam is scattered by the particles and returns to the emitted sensor. The position and velocity information are evaluated respectively from the detected time-of-flight and the Doppler-shift frequency. The nearly instantaneous one-dimensional velocity profile along the beam is obtained. The UVP system could get 1024 data for 40s and at 128 spatial points along the beam. We applied the UVP to the velocity measurements at the gap of the D/P where the PIV was hard to be applied.

3. RESULTS & DISCUSSIONS

3.1 Flow Field in Geometry based on Original Design

In the visualization in the 1/10th scaled model, the gas entrainment at the free surface did not occurred under the same velocity condition. These results show that the D/P is effective to suppress the gas entrainment. However, it was seen that

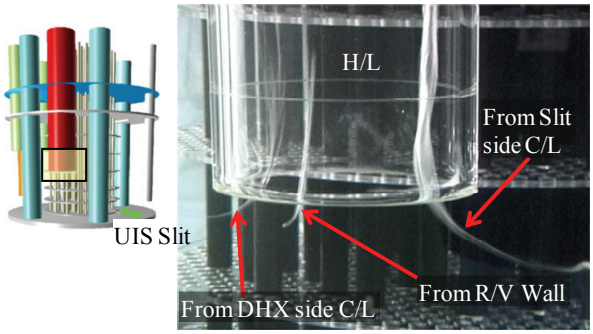

Figure 5 Visualized Image of Vortex Cavitations near H/L Inlet.

three circulations were generated at the neighborhood of the H/L intake. It was observed that three vortices developed to the vortex cavitations as the inlet velocity of the H/L increased. Figure 5 shows the visualized image of the vortex cavitations at the neighborhood of the H/L intake. The inlet velocity of the H/L was 7.3m/s. Three vortex cavitations were observed; one stretched from the R/V wall to the H/L, the other two were from the both C/Ls. It was considered that the vortex cavitations occurred due to the reduction of the pressure at the center of the vortex enhanced by the very high velocity of the H/L inlet (9.2m/s under full power condition). The cavitations generally have the potential to damage the structural components. The suppression of the cavitations is needed to maintain the structural safety. Static pressure is an important factor to estimate the cavitation. However, there is large difference of gas pressure above the free surface between the model and the reactor. The cover gas pressure is 0.25MPa in the reactor and 0.1MPa in the model (open to atmosphere). Thus, the cavitation factor, k, was used to estimate the onset condition of the vortex cavitation in the reactor. The cavitation factor is defined as follows;

$$k = \frac{P - P_s}{0.5\rho v^2} \qquad (2).$$

Here the cavitation factor was defined using the averaged velocity in the H/L at the onset of the vortex cavitation. The cavitation factor (12.8) of in the experiment was approximately 1.6 times larger than that (8.1) under the full power condition of the reactor for the vortex cavitation between the R/V wall and the H/L inlet. This means that the vortex cavitation will occur in the reactor.

3.2 Flow Optimization in Upper Plenum

First of all, we examined the suppression of vortex cavitations. In a design of pump sump, the vortex cavitations have been considered at the intake. The vortex cavitation gives the impeller damage when the cavitation reaches the pump impeller. Some flow control components were investigated in order to prevent the vortex cavitation by the JSME (1984). The JSME standard (JSME, 1984) shows several components, those have the effect to split the flow and to intercept the circulation. One of the components to suppress the cavitation is a vertical rib attached at the wall just behind the pump intake. In our experiment, the vortex cavitation between the R/V wall and the H/L inlet occurred under the lowest velocity condition in the H/L inlet in comparison with the other vortex cavitations. So we set a vertical rib on the R/V wall near the H/L inlet to restrict the rotating flow between the R/V wall and the H/L inlet. Figure 6 shows the configuration of the vertical rib. The vertical rib, which is called 'splitter', has a triangle cross-section and $2D_{H/L}$ (=300mm) in length. The rib was set on the R/V wall at the nearest position to the H/L circumferentially and the center was set at the H/L intake vertically. The rib stuck out about a half of the distance between the R/V wall and the H/L pipe from the wall surface.

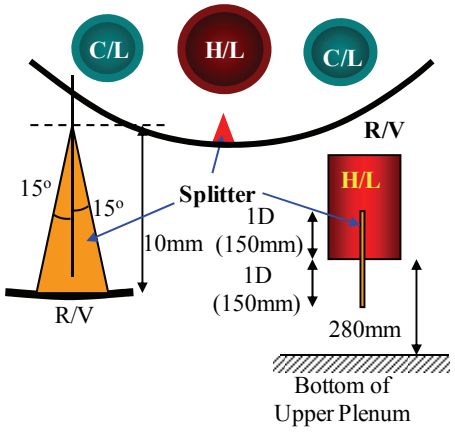

Figure 6 Configuration of Splitter on R/V Wall.

The cavitation factor is 8.1 under the rated condition in the reactor. It is believed that the vortex cavitation will not occur in the re actor when the cavitation factor in the experiment is smaller than 8.1. In the case of the splitter, the cavitation factor was 4.4, which was smaller than the factor in the reactor, at the region

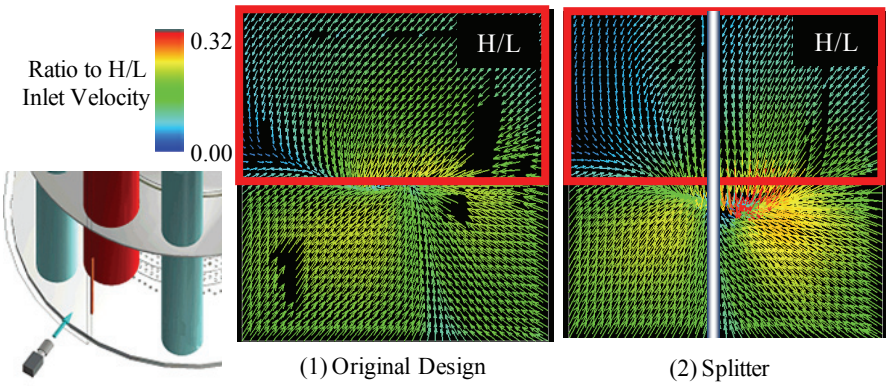

Figure 7 Comparison of Time-averaged Velocity Vectors between Original Geometry and Geometry with Splitter at Region between R/V Wall and H/L.

between the R/V wall and the H/L inlet.

Figure 7 shows the comparison of the time-averaged velocity vectors between the original geometry and the geometry with the splitter at the region between the R/V wall and the H/L pipe. The experimental condition was the Fr number similarity, where the inlet velocity in the H/L was 2.5m/s. In the case of the original geometry, the circulation was observed at the H/L intake. In the case of the splitter, it was shown that the splitter suppressed the horizontal flows above and below the H/L inlet, and also, the vortex was weakened at the height of the H/L intake. In other words, the splitter could reduce sufficiently the circulation near the H/L inlet, which caused the vortex cavitation between the R/V wall and the H/L inlet.

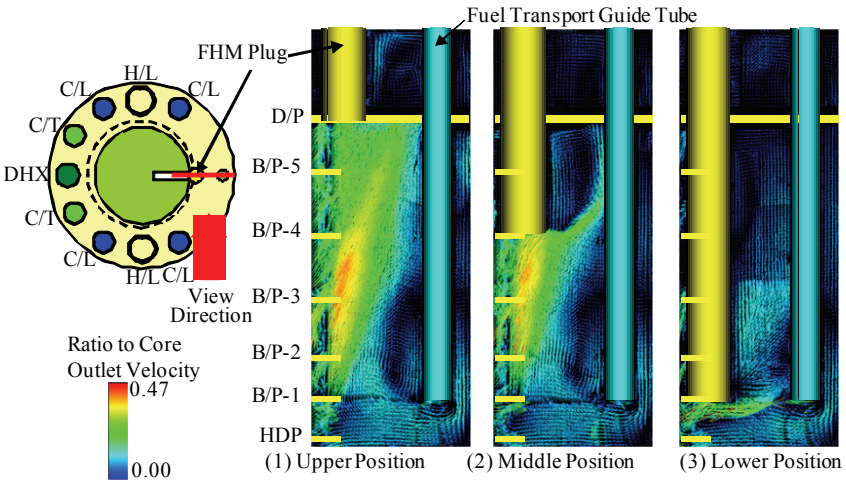

Figure 8 Effect of FHM Plug Height on Flow Fields at Cross Section through UIS Slit.

Next, suppression of the UIS slit jet is considered. The fuel-handling machine (FHM) will be inserted in the upper plenum to exchange the fuel subassembly. There is a hole in the inner D/P to insert the FHM in the design of reactor. The flow passing through the UIS slit would directly impinge on the free surface if the hole was not closed under rated condition in the reactor. Therefore, something to close the hole is needed to reduce the flow velocity toward the free surface. In the design, a plug, which has the nearly same diameter as the FHM (slightly smaller than the hole) and was suspended by the upper deck, has been proposed. In the design, the length of the plug has flexibility as long as the plug is below the D/P. The plug is set in front of the UIS slit. Thus, the plug has a possibility to block the inclined upward flow through the UIS slit to the outer D/P, when the plug is extended to middle or lower position in the R/V upper plenum. And also, the plug will affect the vortex cavitations via the downward flow near the H/L, which was originally coming from the slit jet.

Figure 8 shows the effect of the height of the plug, which fills in the D/P hole for the FHM, on the flow fields at the vertical cross section through the UIS slit obtained from the PIV. The height of the plug was changed to upper, middle and lower positions in the R/V upper plenum. The upper, middle and lower positions meant that the bottom of the plug was set at the heights of the undersurface of the D/P, the fourth B/P and the first B/P, respectively. The experimental condition was the Froude number similarity. In the case of the upper position of the plug, the flow passing through the slit reached the D/P. In the case of the middle position of the plug, it was seen that most of slit jet struck just the bottom of the plug and was turned to horizontal direction. Therefore, the slit jet did not reach the D/P. In the case of the lower position of the plug, the slit jet flowed along the bottom of the plug in radial direction. It may be better to insert the plug deeply in the upper plenum in order to reduce the velocity of the slit jet. However, it was observed that the upward flow along the center side wall of the plug increased in the case of the lower position of the plug.

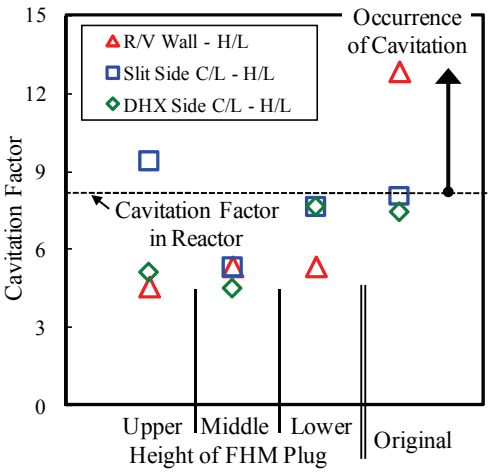

Figure 9 Effect of Plug Height on Cavitation Factors at Onset Condition of Cavitation.

Figure 9 shows the effect of the height of the plug on the cavitation factors based on the inlet velocity in the H/L at the onset condition of the vortex cavitation. In the cases except for the upper position of the plug, it was shown that the obtained cavitation factors were smaller

than that in the reactor. In the case of the middle position of the plug, the factors had the largest tolerance. It is desired that the plug is set at the middle position in the upper plenum to suppress the vortex cavitations near the H/L inlet.

3.3 Evaluation on Onset Condition and Dominant Factors for Gas Entrainment

In the visualization, the gas entrainment did not occur under the velocity similarity condition as the reactor. Therefore, the velocities and the water level were varied widely to obtain the occurrence map and pick the dominant factors out for the gas entrainment.

In the extreme condition, where was far from the rated condition in the reactor, two kinds of the gas entrainment were observed. One occurred at the wake region of the C/L pipe in the UIS slit side under the very large circumferential velocity condition. The vortex, which occurred at the wake region of the C/L pipe when the circumferential flow passed through the C/L pipe, was a potential source of the gas entrainment. Thereto the local downward velocity was generated around the H/L pipe when the circumferential flow impinged to the H/L pipe. It was suggested that the synergy effect between the wake vortex and the local downward velocity induced the gas entrainment at the wake region of C/L pipe. The shape of gas core was rolling and churned temporally. This large variation of gas core made gas bubbles break away from the gas core. Almost of the gas bubbles returned to the free surface and were not sucked into the gap of D/P. The other kind of gas entrainment occurred at the gap between the R/V wall and the H/L pipe under the low water level and the large downward velocity at the D/P gap condition. It was suggested that this gas entrainment took place due to an interaction between the vortex and the downward flow at the D/P gap. The gas core was formed of long-stretched tip. The lifetime of this type of gas core was longer than that at the wake region of C/L. The separation of bubbles occurred in the case where the bubble broke away from the tip of developed gas core or the stretched gas core was chopped off at the midpoint of gas core. Almost of the separated bubbles reached to the D/P gap. It means that the downward flow took place at the neighborhood of the gas core. Of course, it was also observed that the stretched gas core extended to the gap of D/P directly. This kind of gas entrainment was observed in the case where the water level was low or the downward flow at the D/P gap increased.

Figure 10 shows the occurrence map of gas entrainment based on the circumferential velocity and the water level. The horizontal axis is the ratio of the circumferential velocity to the reactor condition and the vertical axis is the ratio of the water level to the equivalent level in the reactor condition. The value of unity in both ratios corresponds to the reactor condition. The red-colored (closed) symbols show the occurrence of gas entrainment and the open symbols show the no occurrence of gas entrainment. In the map, the reactor condition was far from the occurrence condition of the gas entrainment and it is highly unlikely that the gas entrainment occurs in the reactor. The gas entrainment at the wake region of C/L (see blue background area) was independent of the water level

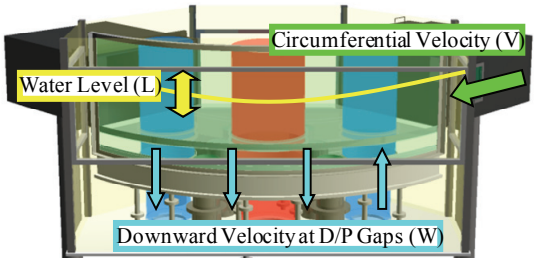

Ratio of Downward Velocity	Occurrence	No Occurrence
1.0	◆	◇
1.5	■	□
2.0*	▲	△
4.0*	●	○

*Ratio was fixed to one at center region of gap between R/V and D/P due to limitation of test apparatus.

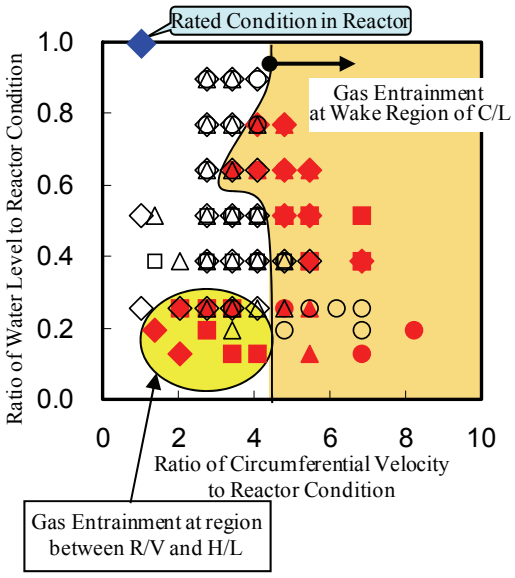

Figure 10 Occurrence Map of Gas Entrainment. (Circumferential Velocity – Water Level)

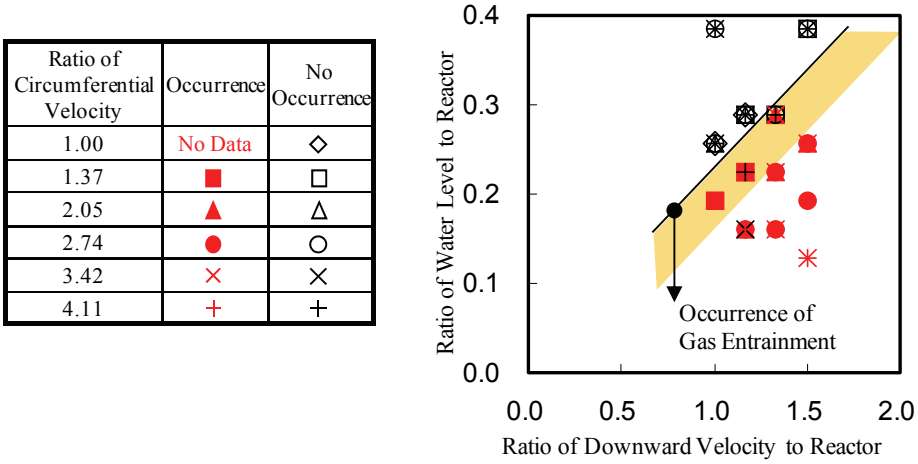

Figure 11 Occurrence Map of Gas Entrainment at Region between R/V and H/L. (Downward Velocity – Water Level)

and occurred under the condition where the circumferential velocity was more than four times larger than that in the reactor. Therefore it was seen that the circumferential velocity was a critical dominant factor for the gas entrainment at the wake region of C/L.

As for the gas entrainment at the region between the R/V wall and the H/L pipe, on the other hand, the occurrence of gas entrainment was limited to the low water level condition and it was observed that the gas entrainment was difficult to take place under the large circumferential velocity condition. Figure 11 shows the occurrence map of gas entrainment based on the downward velocity at the D/P gap and the water level. This map focused attention on the gas entrainment at the R/V-H/L region only. The horizontal axis is the ratio of downward velocity to the reactor condition and the vertical axis is the ratio of the water level to the equivalent level in the reactor condition. The types of the symbols are the same as in Fig. 10. In Fig. 11, it was found that the gas entrainment occurred as the downward velocity increased and the water level decreased. The threshold line of the gas entrainment appeared to the linear line against the downward velocity and the water level. In the experimental results, the equation of threshold line could be expressed as follows:

$$L \approx 0.23 \cdot W \qquad (3).$$

Here L is the ratio of the water level to the equivalent level in the reactor condition and the W is the ratio of the downward velocity to the reactor condition. Eq. (3) shows that W/L was constant for the occurrence of the gas entrainment. The onset condition of gas entrainment was as follows:

$$W/L \geq 4.4 \qquad (4).$$

The downward velocity is equal to zero at the free surface and the W is defined as the velocity at the top of D/P. Therefore W/L corresponds to the vertical gradient of downward velocity in a macroscopic model. Consequently, it was found that this kind of gas entrainment occurred under the condition where the normalized velocity gradient in vertical direction was more than 4.4.

As for the gas entrainment at the region between the R/V and the H/L pipe, almost of the bubbles separated from the tip of the gas core reached to the D/P gap. Therefore this type of the gas entrainment was needed to evaluate the mechanism of occurrence. Figure 12 shows the flow pattern at the region between the R/V wall and the H/L pipe under the condition shown in Table 1 (2). The left hand side picture shows the visualized image using a halogen lamp. The right hand side figure shows the instantaneous velocity vectors in horizontal cross section at the same time as the visualized image. These images were taken when the gas core length was maximized. The gas core in the left image corresponded to the center of vortex in the right figure. In the velocity vectors, strong flow along the R/V wall was observed. It was presumed that this flow was formed on the ground that the circumferential flow from the UIS slit passed through the region between the H/L and the C/L in the DHX side and toward the R/V wall, and some of this flow ran along the R/V wall. On the other hand, the flow was nearly stagnant in the neighborhood of the H/L pipe. The free surface vortex developed from this shear flow at the region where two kinds of flows met.

In the experimental result, the gas entrainment took place due to the development of the vortex at the free surface. This vortex was caused by the shear flow at the region between the R/V wall and the

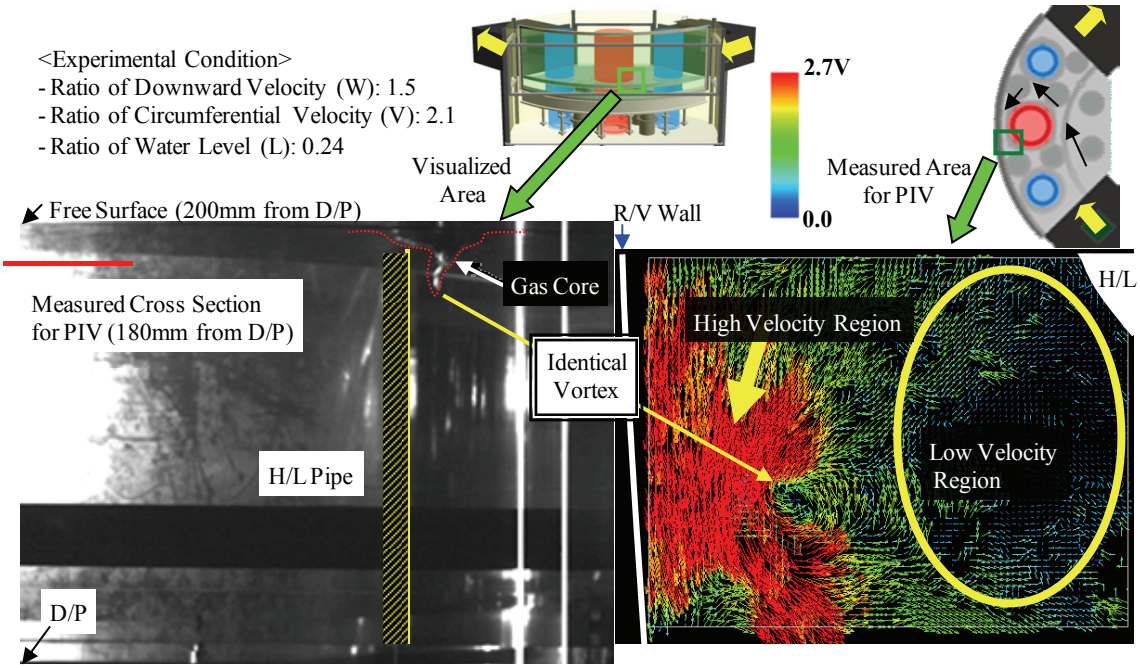

Figure 12 Flow Pattern at Region between R/V and H/L.

H/L pipe. The vortex developed and the gas entrainment occurred in the case where the downward flow increased.

4. CONCLUSIONS

An innovative sodium cooled fast reactor has been investigated as the FaCT project in JAEA. Remarkable characteristics of the upper plenum in the reactor vessel (R/V) are the increase of the velocity and the adoption of a column type upper inner structure (UIS) with a radial slit for the fuel-handling machine (FHM). We performed an 1/10th scale water experiment for the upper plenum of the R/V in order to evaluate hydraulic phenomena, to extract the hydraulic problems and to optimize the flow field. Furthermore, we carried out the large scale partial model which simulated the upper plenum at the neighborhood of the free surface with 1/1.8th scale in the reactor in order to evaluate the gas entrainment. The experimental results were as follows.

Gas entrainment at the free surface did not occur within the velocity range in the 1/10th scaled model. These meant that the dipped plate (D/P) worked against the gas entrainment. However, three vortex cavitations were observed at the neighborhood of the H/L inlet. One stretched from the R/V wall, the other two stretched from the both C/Ls. The cavitation factors, which were obtained from the average velocity in the H/L at the onset condition of the cavitation, showed that the reactor would have the cavitation. It is needed to suppress the vortex cavitations in order to keep the structural safety.

As for the vortex cavitation from the R/V wall, which was easier to occur, the vertical rib was set on the R/V wall at the closest position to the H/L pipe to restrict the rotating flow near the H/L inlet. It was shown that the vortex cavitation between the R/V wall and the H/L inlet did not occur under the same cavitation factor (8.1) as in the reactor. The cavitation factor at the onset condition was reduced from 12.8 to 4.4 by the splitter.

In order to reduce the flow through the UIS slit, a FHM hole in the D/P in front of the UIS slit was closed by the plug with the cylindrical shape. The parameter was plug length (height of the bottom of plug). In the case of the middle or the lower plug position in the upper plenum, the jet impinging to the D/P was suppressed in comparison with that in the case of the higher plug position. In these cases, in addition, the vortex cavitation was not broken out anywhere under the same cavitation factor as in the reactor.

In the cases where the velocities and the water level were varied, two kinds of gas entrainment took place. One occurred at the wake region of C/L pipe in the UIS slit side under the condition where the circumferential velocity was more than four times of the reactor condition. The other one occurred at the region between the R/V wall and the H/L pipe under the condition where the normalized velocity gradient in vertical direction was larger than 4.4. Here the normalized velocity gradient was defined as the ratio of the non-dimensional downward velocity to the non-dimensional water level.

At the region between the R/V wall and the H/L pipe, on the other hand, it was found that the shear flow, which was based on the interaction between the strong flow along the R/V wall and the stagnant flow at the neighborhood of H/L, caused the gas entrainment from the simultaneous measured results of the visualization of gas core and the local velocity.

Consequently, there is a chance for this design of the compact reactor vessel to suppress the gas entrainment and vortex cavitation.

NOMENCLATURE

C/L : Cold Leg (pipe)
D/P : Dipped Plate
Fr : Froude number
G : Gravity (=9.81m/s^2)
H/L : Hot leg (Pipe)
k : Cavitation factor
L : ratio of water level in experimental condition to that in reactor condition
P : Pressure (N/m^2)
Ps : Saturated vapor pressure of fluid (N/m^2)
Re : Reynolds number
R/V : Reactor Vessel
UIS : upper inner structure
V : Velocity (m/s)
W : ratio of downward velocity in experimental condition to that in reactor condition
ρ : Density of fluid (kg/m^3)

REFERENCES

R. J. Adrian, “Particle-imaging techniques for experimental fluid mechanics”, *Ann. Rev. Fluid Mech.*, Vol.23, pp.261 (1991).

Y. Eguchi et al., "Experimental study on scale effect on gas entrainment at free surface", N*uclear Engineering and Design*, Vol.146, pp.363-371 (1994-1).

Y. Eguchi et al., “Gas entrainment in the IHX vessel of Top-Entry Loop-Type LMFR”, *Nuclear Engineering and Design*, Vol.146, pp.373-381 (1994-2).

JSME, *Standard Method for Model Testing the Performance of a Pump Sump*, JSME Standard (JSME S 004), Maruzen, Tokyo, Japan (1984) (in Japanese).

N. Kimura et al., “Noise Reduction Techniques for the Particle Image Velocimetry -Application to an Experimental Study on Natural Convection in a Fast Reactor Core-“, *Proc. of 8th International Conference on Nuclear Engineering*, Baltimore, MD, USA, April 2-6, ICONE-8405 (2000).

S. Kotake et al., “Development of Advanced Loop-Type Fast Reactor in Japan (1): Current Status of JSFR Development”, *Proc. of the 2008 International Congress on the Advances in Nuclear Power Plants*, Anaheim, CA, USA, June 8-12, ICAPP’08-8226 (2008).

J. Sakakibara et al., “Measurements of Thermally Stratified Pipe Flow using Image Processing Techniques”, *Exp. in Fluids*, Vol.16, pp.82-96 (1993).

Y. Shimakawa et al. “Innovative Concept of the Sodium-Cooled Reactor to Persue High Economic Competitiveness”, *Nuclear Technology*, Vol.140, pp.1-17 (2002).

Y. Takeda, “Development of an ultrasound velocity profile monitor”, *Nuclear Engineering and Design*, Vol.126, pp.277-284 (1990).

T. Ueta et al. “The Development of Demonstration Fast Breeder Reactor (DFBR)”, *Proc. of 4th International Conference on Nuclear Engineering*, Kyoto, Japan, April 23-27, Vol.2, pp.771 (1995).